Journal of the European Ceramic Society 16 (1996) 687–694

0955-2219(95)00190-5
0955-2219/96/$15.00

# Influence of Grain Size on the Toughness and Thermal Shock Resistance of Polycrystalline $YBa_2Cu_3O_{7-\delta}$

F. Osterstock,[a,*] I. Monot,[b] G. Desgardin[b,†] & B. L. Mordike[a]

[a]Institut für Werkstoffkunde und Werkstofftechnick, TU Clausthal, 38678 Clausthal — Zellerfeld, Germany
[b]Laboratoire CRISMAT — CNRS URA 1318 — ISMRA — Université de Caen, Boulevard du Maréchal Juin 14050 Caen Cedex, France

(Received 3 November 1994; revised version received 16 October 1995; accepted 24 October 1995)

***Abstract***

*The toughness and thermal shock resistance (quenching from RT in air into liquid nitrogen) have been investigated on four grades of polycrystalline 'YBaCuO' of almost equal porosity using the Vickers indentation technique. The mean grain sizes varied from 1·5 to 10 μm. The change in toughness with increasing grain size is described by a bell-shaped curve as already published by Rice* et al. *for the case of other non-cubic ceramics. For the determination of the thermal shock resistance, an original method, based on the relative increase of the length of Vickers indentation radial cracks, as the sample is quenched, has been used. The ranking of the four grades can only be explained if the increase of the thermal residual mismatch stresses, as the samples are put into liquid nitrogen, is taken into account such as to predict a shift of the bell-shaped change of toughness with increasing grain size as the temperature reaches that of liquid nitrogen. The proposed methodology delivers a powerful tool for investigating non-cubic polycrystalline structural or functional ceramics in the R&D stage.*

*Nous avons utilisé la technique de l'indentation Vickers pour étudier la tenacité et la résistance au choc thermique (trempe de la température ambiante à l'air dans l'azote liquide) de quatre nuances de 'YBaCuO' polycristallin et de porosités semblables. Les tailles moyennes des grains varient de 1·5 à 10 μm. La variation de la tenacité lorsque la taille des grains augmente suit une forme en cloche, telle que celle proposée par Rice* et al., *pour d'autres céramiques non-cubiques. Une méthode originale, basée sur l'augmentation relative de la longueur des fissures radiales de l'indentation Vickers lorsque l'échantillon est trempé, a été utilisée pour déterminer la résistance au choc thermique. Le classement des quatre nuances nécessite la prise en compte d'un accroissement des contraintes thermiques résiduelles entre les grains lorsque les échantillons sont refroidis dans l'azote liquide. Ceci permet de proposer un décalage de la courbe en cloche qui décrit la variation de la tenacité avec la taille des grains lorsque le matériau atteint la température de l'azote liquide. La méthodologie proposée se révèle comme un bon outil pour l'étude de céramiques fonctionnelles ou structurales à structure non-cubique dans le stade de recherche et développement.*

*Die Bruchzähigheit und der Thermoschockwiderstand (Abschrecken von Luft bei Raumtemperatur in flüssigen Stickstoff) wurden an vier vielkristallinen 'YBaCuO' Sorten von beinahe gleicher Porosität, mittels der Vickershärteeindrucksmethode untersucht. Die mittlere Korngrösse varierte zwischen 1·5 und 10 μm. Die Anderung der Bruchzähigheit mit steigender Korngrösse wird durch eine glockenartige Kurve beschrieben, wie schon von Rice* et al., *für andere nicht-kubische Keramiken vorgeschlagen. Der Thermoschock-widerstand wurde mittels einer Methode, die auf der relativen Verlängerung der Vickerseindruck-risse während des Abschreckens beruht, untersucht. Zur Einordnug der vier Sorten muss die Zunahme der thermischen Eigenspannungen zwischen den Körnern während des Abhühlens in flüssigem Stickstoff in Betracht gezogen werden. Dies hat eine Verschiebung der glockenartigen Anderung der Bruchzähigkeit mit steigender Korngrösse bei der Temperatur des flüssigen Stickstoffs zur Folge. Die vorgeschlagene Methodik erweist sich als sehr angebracht für die Untersuchung von vielkristallinen nicht-kubischen Funktions-oder-Baukeramiken in der Entwicklungsphase.*

*This work was done during the time F. Osterstock was on leave from LERMAT — CNRS URA 1317 — ISMRA.
† To whom correspondence should be addressed.

## 1 Introduction

Although much attention is currently paid to the fabrication of high-temperature superconducting materials, either in the shape of thin films or being textured, a potential still exists for the use of polycrystalline ones. It has been recognised very early that, for the latter, the grain size plays an important role in the density of the critical current.[1,2] Microcracking along the grain boundaries under the action of thermal mismatch stresses is a common feature of non-cubic functional and structural polycrystalline ceramics. However the grain sizes for which a dramatic decrease in critical current density has been detected by Refs 1 and 2 differ. This reveals a general problem of grain boundary engineering about which it has been speculated for this family of materials[3,4] or in a more general way.[5]

It appears from these works that the quality of a grain boundary is often best approached by the grain boundary energy, $\gamma_{gb}$, which describes its mechanical resistance, but also depends on the geometrical orientation of the two neighbouring grains on the one hand and on the nature and amount of impurities located in it on the other hand. The latter also influence the quality and the coherency of the superconducting domains.

Furthermore the mechanical resistance of 'YBaCuO' and other high-$T_c$ superconducting cuprates is only poorly documented. In addition to the determination of usual mechanical properties,[6,7] the indentation method has been used for the measurement of more specific properties[8,9] of single crystals or of polycrystals.[10] The latter encompasses the toughness which provides more reliable information on the quality of a sintered microstructure than the single rupture stress which depends on the size of the largest defect and is thus inadequate for judging materials in the state of research and development. Also the toughness appears in treatments of thermal shock resistance, which is of importance when the functional part is cooled from room temperature to that of liquid nitrogen.

In the present paper, the indentation method has been used to determine toughness at room temperature and thermal shock resistance of polycrystalline YBaCuO when quenched into liquid nitrogen, as a function of grain size. Existing models are used in order to discuss the experimental results.

## 2 Materials and Experimental Procedures

Mixtures of $Y_2O_3$, CuO and $BaCO_3$ have been calcinated at 880°C, then milled and calcinated again and remilled. The resulting powders were then uniaxially pressed at room temperature and subsequently pressureless sintered at 920°C in air such as to yield various grain sizes.

Afterwards the resulting discs (5 mm in thickness and 25 mm in diameter) were refired and then ground and polished to remove the outer skin, which may have been fitted with thermal stresses of the first kind, and for metallographical purposes. The density of these discs was measured using Archimedes' principle in toluol. Four different microstructures were obtained; their characteristics are given in Table 1 in addition to the toughness as it will be deduced below. Electron scanning micrographs are shown in Fig. 1 in order to see the microstructures under investigation.

Thoughout this study, the indentation method was used for determining the toughness and evaluating the thermal shock resistance with the help of Wolpert and Zeiss durometers. Details will be given below concerning the working-out scheme

**Table 1.** Designation of the samples and main characteristics

| *Sample* | *920 B* | *920 C* | *920 D* | *920 A* |
|---|---|---|---|---|
| $\mu$ structure | Very fine | Fine | Medium | Coarse |
| Porosity vol.% | 19 | 19 | 22 | 16 |
| $K_c$, MPa $\sqrt{m}$ | 0·70 | 0·84 | 1·64 | 0·24 |
| Grain size, $\mu$m | 1·5 | 3·5 | 5·5 | 10 |

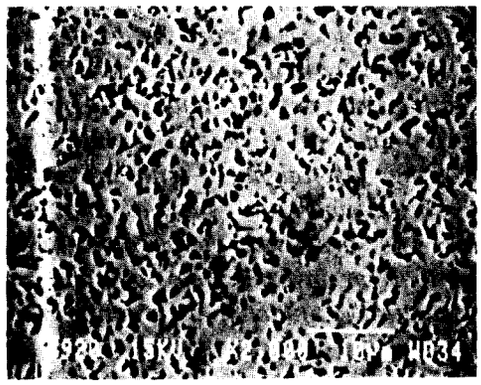

(a)

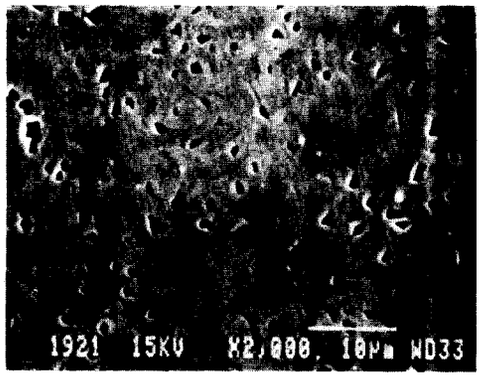


(b)

**Fig. 1.** Electron micrographs of samples 920B (a) and 920A (b)

and procedures, A well defined procedure was used for determining the toughness, via the direct crack length measurement method.[11] Thermal shock was realized in putting as-indented samples into liquid nitrogen, within a Dewar. Care was taken during reheating to avoid condensation of ambient humidity, which may cause sub-critical crack extension due to stress enhanced corrosion, in isolating the sample into water absorbing paper after it had been swept a first time. This also reduced the reheating rate.

## 3 Results

### 3.1 Toughness using the Vickers indentation method

The procedure used here is that initially outlined by Anstis *et al.*[11,12] Due to the elasto-plastic mismatch between the deformed zone under the indentor and the remaining elastic matrix a symmetric crack pattern appears during unloading the Vickers diamond. These cracks are in equilibrium between the residual central opening and the toughness, $K_c$ of the material. Such a pattern is shown in Fig 2; Fig. 3 gives details concerning the parameters used. A dimensional analysis yields a relation between indentation load, $P$, crack length, $c_0$, and the toughness:

$$K_c = \xi(E/H)^{1/2} \cdot P \cdot c_0^{3/2} = \chi r \cdot P \cdot c_0^{-3/2} \qquad (1)$$

where: $E$ is Young's modulus and $H$ the hardness; $\xi$ and $\chi r$ are dimensionless proportionality factors, with:

$$\chi r = \xi(E/H)^{1/2} \qquad (2)$$

Values of the microhardness $H_v$ = 8·7 GPa[8] and Young's modulus $E$ = 180 GPa[6] were used to verify whether the ratio $(EH)$ fits with the values used by Anstis *et al.*[11,12] They obtained $(E/H) \approx 30$ for a range of glassy and crystalline materials, whereas $(E/H) \approx 20$ holds in the present case. Thus toughness was deduced from:

$$K_c = 0{\cdot}77\ P \cdot c_0^{-3/2} \qquad (3)$$

despite the fact that porosity may yield densification before plastic deformation occurs beneath the indentor. Furthermore, as can be deduced from the scatter of the Young's moduli published by Alford *et al.*[6] the value of the Young's modulus of the bulk may depend on grain size due to thermal mismatch stress induced microcracking of the grain boundaries. The values of the proportionnality factors may thus vary with grain size too. The purpose of this paper is however to underline the resulting behaviour.

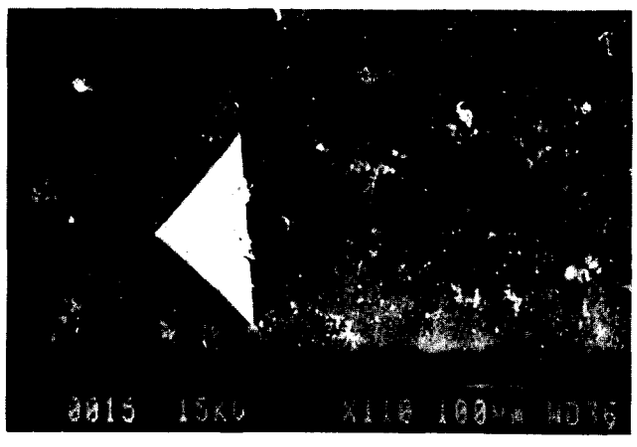

Fig. 2. Electron micrograph of a Vickers indentation and associated radial cracks in grade 920D.

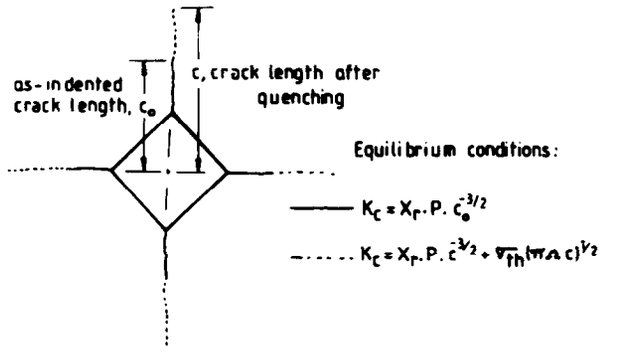


Fig. 3. Schematic of the Vickers indentation induced median-radial crack system, its extension during quenching and the associated parameters. In the quenching it has been assumed that the indentation crack system is located within a skin of homogeneous and constant peak stresses.

A comparison has been made between the medium grain-sized grade 920 D and three materials for which the indentation crack system is already well established: Palmquist cracks for WC–Co and the median-radial crack system for $Al_2O_3$ and SiC. The former is characterized by the fact that a level of indentation load is needed for the occurrence of the first crack, whereas for the latter the identation load versus radial crack length plot passes the zero point in accordance with eqn (1). It can be seen in Fig. 4 that the YBaCuO 920 D follows the behaviour of a median-radial crack system.

In Fig. 5, the results of the four grades are plotted and compared with $Al_2O_3$ ($K_c$ = 3·5 MPa Vm) and SiC ($K_c$ = 3·2 MPa Vm) in a $P^{2/3}$ versus $c_0$ plot. This coordinate system, $P^{2/3}$ versus $c_0$, has been chosen, because, as can be deduced from eqn (1), the slope is directly proportional to $K_c^{2/3}$, and, in addition to the verification made just above, it is less subject to errors than measurements made with only one indentation load. The values of $K_c$ deduced in this way are given in Table 1 and plotted as a function of grain size in Fig. 6. As can be seen, as grain size increases, the toughness first increases and then decreases. This is a feature which has already been observed for non-cubic

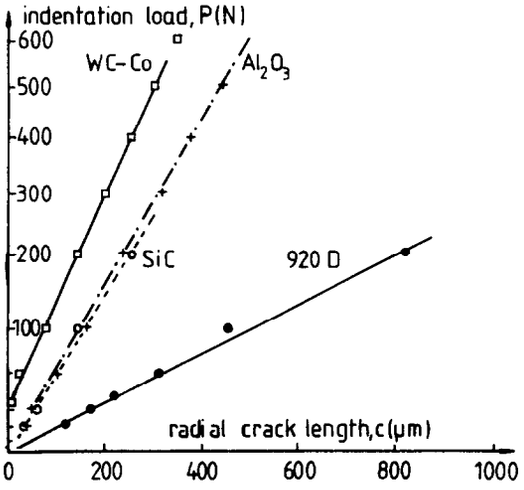


**Fig. 4.** Indentation load versus radial crack length plots for a material exhibiting Palmquist cracks (WC–Co) and others exhibiting a median-radial crack system (SiC, $Al_2O_3$ and YBaCuO).

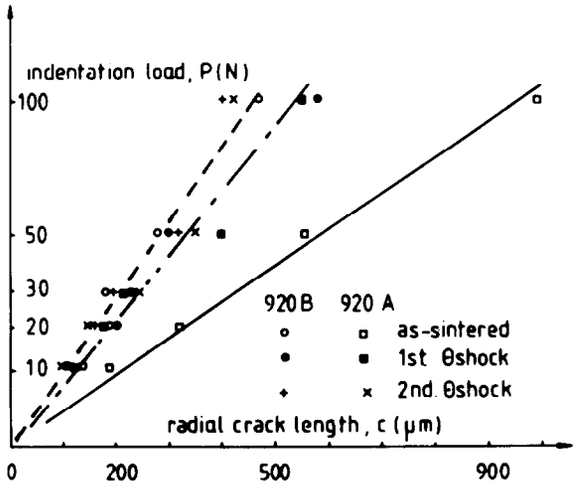


**Fig. 5.** Indentation load versus radial crack length for the four grades of YBaCuO and comparison with SiC and $Al_2O_3$.

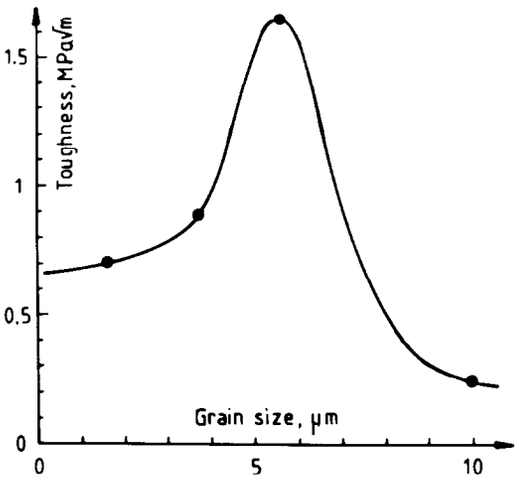


**Fig. 6.** Variation of Vickers indentation toughness with grain size for the four YBaCuO grades.

ceramics[13–15] and will be discussed later in conjunction with the results of thermal shock testing. The maximum value of $K_{1c}$ is detected at a grain size of about 6 $\mu$m which is much larger than the value of 1 $\mu$m computed by D. R. Clarke *et al.*[3] for spontaneous microcracking of polycrystalline YBaCuO. This discrepancy may be due to the values of the toughness of the grain boundaries which are higher than that used in ref. 3. Additionally, the polycrystalline YBaCuO investigated here is porous, thus lower values of the residual thermal mismatch stresses are expected.

### 3.2 Thermal shock resistance

High-temperature ceramic superconductors are aimed to be put to work at the temperature of liquid nitrogen and because an in-between stage at room temperature is technically necessary, the investigation and the knowledge of the resistance against sudden temperature changes are necessary. Since the works of Buessen[16] and Kingery[17] many efforts have been devoted to the thermal shock resistance of structural ceramics.[18] These approaches, however, propose to rank the materials in determining a critical quenching temperature difference, $\Delta T_c$, following a method which needs a large number of specimens having the same microstructure. This is hardly achievable for materials in the R&D stage and, in the case investigated here, the relative resistance of materials against given quenching conditions is looked for. For this purpose a test based on the conditions of the stable extension of Vickers indentation cracks has been developed[19,20] and will be briefly outlined below.

The principle is based on the existence of residual contact stresses which act as a central opening force, or wedge, such as to extend the radial cracks until its driving force is counterbalanced by the crack resistance of the indented material (eqn (1)). Now if an external stress of mechanical or thermal origin $\sigma_{th}$ is added to this wedge effect, the indentation cracks increase their size, $c$. The critical stress intensity factor is then:[11,12]

$$K_c = \chi r \cdot P \cdot c^{3/2} + \sigma_{th}(\pi \Omega c)^{1/2} \qquad (4)$$

It corresponds to the superposition of the residual indentation stress intensity factor and that due to the external stress, $K_e = \sigma_{th}(\pi\ \Omega\ c)^{1/2}$ where $\Omega$ is a geometrical factor taking into account the shape and size of the semi-elliptical surface cracks ($\Omega$ = 0·405) The occurence of a negative and a positive exponent for the actual radial crack length, $c$, indicates the possible existence of stable crack extension during the superimposition of stresses given above. The differentiation of $\sigma_{th}$ with respect to the actual crack length, $c$, shows that stable crack growth occurs between the initial, or as-indented (see Fig. 7), crack length, $c$, and a given crack length, $c_m$ Both depend on the indentation load, $P$, and on the material toughness, $K_c$ The value of $c_m$ is obtained as:

$$c_m = (4\chi r \cdot P/K_c)^{2/3} \quad (5)$$

in conjunction with a stress level, $\sigma_m$; both defining the end of stable and the onset of uncontrolled crack extension:

$$\sigma_m = 3K_c/4((\pi\Omega c_m)^{1/2} \quad (6)$$

These bell-shaped curves are schematically shown in Fig. 2 of ref. 2 and reproduced for several indentation loads in Fig. 7. The aim is to show how indentation cracks due to different indentation loads increase in length for a given external applied stress, which is the peak of the thermal transient stress, $\sigma_{th}$ in the present case. For a value of the applied stress, $\sigma_{th} = 0$, the radial cracks have their initial length, $c_o$ (eqn (3)). In Fig. 7, a level of $\sigma_{th} = 58$ MPa has been arbitrarily chosen such as to correspond to a maximum of one of the curves ($P$=100 N). It shows that the radial cracks extend in a stable, and then possible unstable way, depending on the indentation load, as shown by the thick parts of the bell-shaped lines. It is a special case, since it defines the conditions for the onset of unstable extension as the curve describing the behaviour of a crack system obtained with an indentation load of $P$ = 100 N where the crack length attains $c = c_m$. The ratio $c_m/c_0$ is 2·52, independently of the indentation load.

Values of $c/c_o$, the relative increase in radial crack length, can thus be calculated as a function of indentation load, $P$, and for various levels of applied stress and toughness of the materials, $K_c$. Some features are shown in Fig. 8. It appears that the relative increase in radial crack length $c/c_o$, tends as a function of the indentation load, the more rapidly towards $c_m/c_o = 2{\cdot}52$, the higher the level of the applied stress or the lower the toughness of the material.

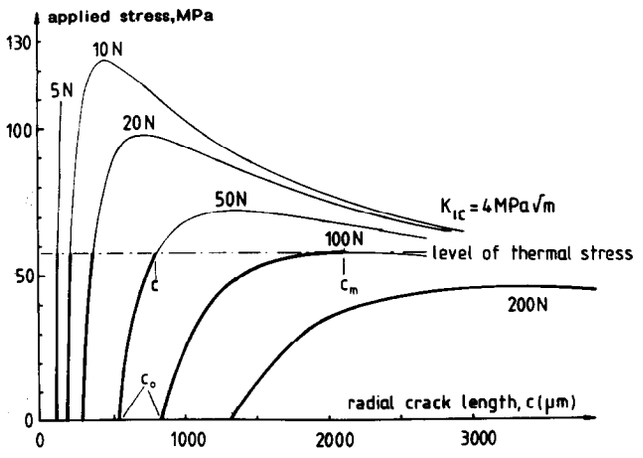


**Fig. 7.** Stable (increasing) and unstable (decreasing) branches of the extension of Vickers indentation radial cracks under the action of an applied stress. The value of the indentation load is given on the top of each curve. The extensions for a given level of applied stress are the thick part of the lines ($\chi r$ = 1).

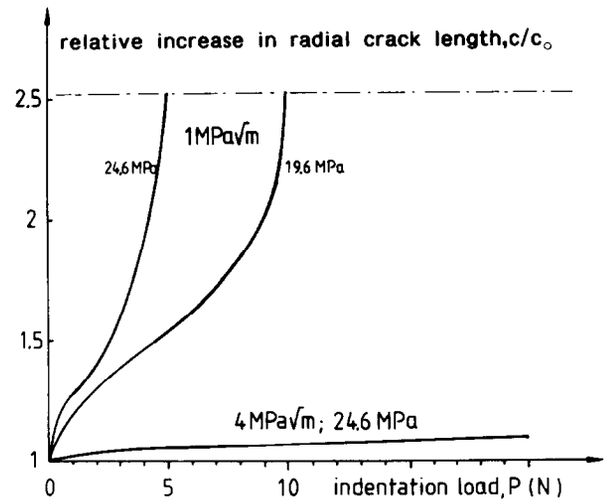


**Fig. 8.** Comparative effects of toughness and given applied, mechanical or thermal stresses on the relative increase in length of the radial cracks from Vickers indentation, as a function of indentation load. The limit of stable and thus measurable crack extension ($c/c_o$ = 2·52) is indicated.

In the present case, since the YBaCuO samples differ only by the grain size and since they have all the same shape and dimensions, it is assumed that the value of the peak of the thermal transient stress, $\sigma_{th}$, appearing when the samples are put into liquid nitrogen, is the same for the four grades. The response of the sample to quenching is thus solely dictated by the toughness and the relative increase in radial crack length, $c/c_o$, is some indicator of the thermal shock resistance.

The experimental results are shown in Fig. 9. It can be seen that the shape of the experimental curves follows that predicted in Fig. 8. From the way these curves have been derived, it means that, the higher or the steeper the curve, the less thermal shock resistant is the material. In the present

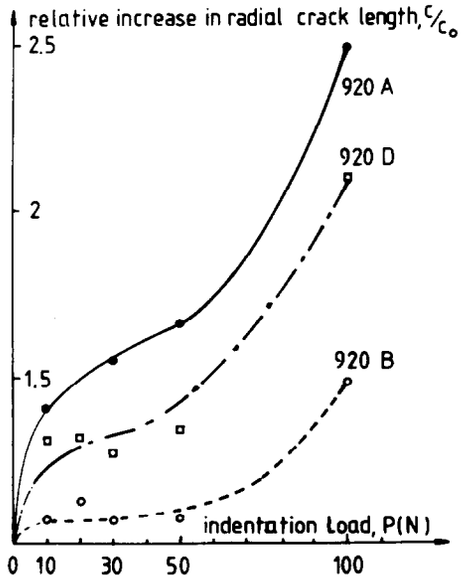


**Fig. 9.** Relative resistances against thermal shock of three YBaCuO grades when quenched from room temperature in air into liquid nitrogen.

case, it shows that the thermal shock resistance decreases with increasing grain size. It can be noted that this ranking is not the same as that for the toughness which exhibited first an increase and then a decrease with increasing grain size. This apparent discrepancy will be discussed on the basis of existing models and results obtained on both functional and structural ceramics.

Further toughness measurements made on quenched samples give some information for speculating on the role of residual thermal mismatch stresses. The state of the residual stresses depends solely on the testing temperature (room temperature in the present case), if they have not been, at least partly, released by spontaneous microcracking, which is an irreversible process. Microcracking during the stage in liquid nitrogen can thus be detected at room temperature through toughness measurements using the indentation method. The results are shown in Fig. 10 for grades 920B (finest grain size) and 920A (coarsest grain size). The toughness of grade 920B did not change after the first, nor after the second quenching, indicating that no microcracking had occurred. Grade 920A behaves differently. After the first quenching a sharp and apparent increase in toughness is observed. A second quenching does not yield further changes. The change observed after these quenchings indicates a change in the internal stress state which may be due to microcracking as detected by other means by D. S. Smith *et al.*[2] and M. Aslan *et al.*[1] The reasons why the release of residual stresses through microcracking yields an apparent increase in toughness are not clear. Previously obtained results on thermally shocked fine-grained alumina[21] and coarse-grained chromium-magnesia refractories[22] indicate opposite changes of toughness after thermal shock. Grade 920A would be in accordance with the refractory. They have also the common features of being porous and coarse-grained. This problem however should be discussed within further papers. An explanation may be that nuclei of microcracks are created which would not have been activated otherwise.

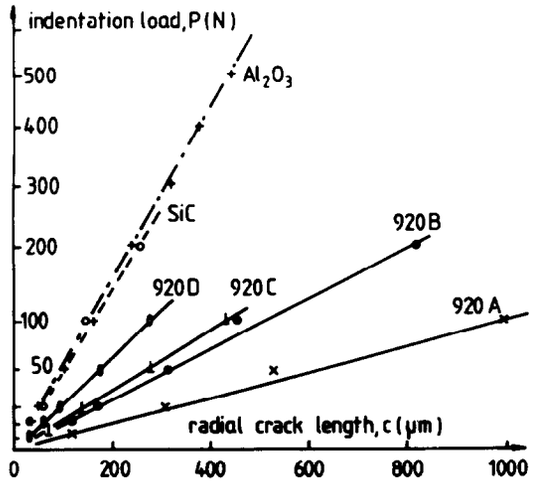


**Fig. 10.** Detection of microstructural damage in the coarse-grained 920A grade after quenching into liquid nitrogen.

## 4 Discussion

The shape of the curve describing the change in toughness with grain size is similar to that already shown by Rice, Freiman, Becher and Pohanka.[13–15] Their model is based on the existence of thermal residual mismatch stresses at the grain boundaries due to the anisotropy of the thermal expansion coefficients. These residual stresses are also investigated for their role in dielectric failures[23,24] and the influence of grain size (the tendency to grain boundary microcracking increases with increasing grain size) has been established[25].

Residual thermal mismatch stresses may enhance toughness. The case must be considered when an external stress is applied and superimposed to these already existing stresses in order to reach the conditions for grain boundary microcracking. Rice and Freiman[14] considered an arithmetic contribution of the grain boundary energy per unit area of primary crack growth. Other models consider the superimposition of applied and residual stresses (stress-induced microcracking) for deriving models of toughness based on the shielding effect of a frontal microcracked, or process zone.[26–28] It appears from these models that as grain size increases, the density of microcracks ahead of the primary crack increases in a first time, enhancing the shielding effect and thus toughness. However above a critical grain size, the strain energy of the grains is high enough that the decrease in applied stress necessary for inducing microcracking counterbalances more and more the shielding effect. Toughness decreases then towards zero for a grain size at which spontaneous microcracking occurs.[23–31]

When the YBaCuO samples are cooled to the temperature of liquid nitrogen (77 K), the residual thermal mismatch stresses and the associated strain energy of the grains, increase with respect to their level at room temperature. This results in a shift, towards smaller grain sizes, of the bell-shaped curve describing the variation of toughness with grain size at room temperature (see Fig. 6). This shift is illustrated in Fig. 11 as well as the expected changes in toughness for a temperature of 77 K.

This shift may explain the apparent discrepancy between the ranking of the toughness measured at room temperature and the ranking of the thermal shock resistance as a function of grain size. Extension of the radial crack during thermal shock

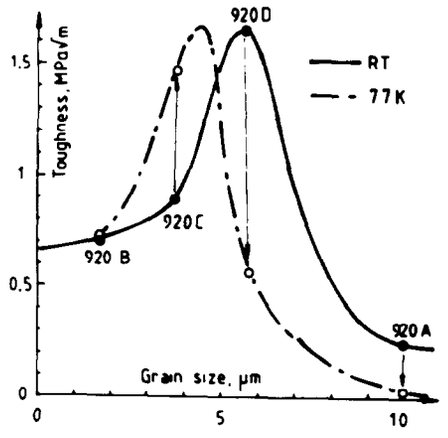


**Fig. 11.** Speculated shift of the toughness versus grain size as testing temperature varies from room temperature to that of liquid nitrogen.

takes place at the temperature of liquid nitrogen and the toughness at that temperature must be considered. The speculated shift may yield the same ranking for the toughness at 77 K and the thermal shock resistance. Unfortunately the lack of testing materials and facilities did not allow of an experimental confirmation.

## 5 Conclusion

In the present work the influence of grain size on the toughness and thermal shock resistance of polycrystalline YBaCuO has been investigated in using the Vickers indentation method. It has been shown that this experimental methodology yields valuable quantitative and qualitative informations on these materials in the R&D stage. The changes of toughness and thermal resistance with grain size can be correlated within the frame of models taking residual thermal mismatch stresses into account.

In view of the discrepancies of published results on the decrease of critical current density with increasing grain size, inquiries on the nature and structure of the grain boundaries should be undertaken in order to become able to tailor microstructures exhibiting both high toughness, thermal and microcracking resistance, as well as satisfactory current densities and reliability.

## References

1. Smith, D. S., Suasmoro, S. & Gault, C., Demonstration of grain growth induced microcracking and its role in the electrical response of $YBa_2Cu_3O_{7-\delta}$. *J. Eur. Ceramic Soc.*, **5** (1989) 81–5.
2. Aslan, M., Jaeger, H., Kaiser, G., Gröner, R., Schulze, K. & Pezow, G., Influence of microstructure on the superconducting properties of polycrystalline $YBa_2Cu_3O_{7-\delta}$. *J. Eur. Ceramic Soc.*, **6** (1990), 129–35.
3. Clarke, D. R., Shaw, Th. M. & Dimos, D., Issues in the processing of cuprate ceramic superconductors. *J. Am. Ceramic Soc.*, **72**(7) (1989) 1103–13.
4. Zhu, Y., Tafto, J. & Suenage, M., Defects in high $T_c$ cuprate superconductors. *MRS Bulletin*, Nov. 1991, 54–9.
5. Clarke, D. R., Grain boundaries in polycrystalline ceramics. *Ann. Rev. Mater Sci.*, **17** (1987) 57–74.
6. Alford, N. McN., Birchall, J. R., Clegg, W. J., Hormer, M. A., Kendall, K. & Jones, D. H., Physical and mechanical properties of $YBa_2Cu_3O_{7-\delta}$ superconductors. *J. Mat. Science*, **13** (1988) 761–8.
7. Ochiai, S., Hayashi, K., Hosoda, A. & Osamura, K., Tensile strength and its scatter of superconducting $YBa_2Cu_3O_{7-\delta}$ in silver sheathed wires and tapes estimated from multiple cracking. *J. Mat. Sci. Letters*, **10** (1990), 117–19.
8. Cook, R. F., Dinger, T. R. & Clarke, D. R., Fracture toughness measurements of $YBa_2Cu_3O_{7-\delta}$ single crystals. *Appl. Phys. Letters*, **51**(6) (1987), 454–6.
9. Fujimoto, H., Murakami, M. & Koshizuka, N., Effect of $Y_2BaCuO_5$ on fracture toughness of YBCO prepared by a MPMG process. *Physica C*, **203** (1992), 103–10.
10. Osterstock, F., Strauss, S., Mordike, B. L., Monot, I. & Desgardin, G., Toughness and thermoshock resistance of polycrystalline $YBa_2Cu_3O_{7-\delta}$. *J. Alloys and Compounds*, **195** (1993), 679–82.
11. Anstis, G. R., Chantikul, P., Lawn, B. R. & Marshall, D. B. A critical evaluation of indentation techniques for measuring fracture toughness; I, Direct crack measurements. *J. Am. Ceramic Soc.*, **64**(9) (1981) 533–8.
12. Chantikul, P., Anstis, G. R., Lawn, B. R. & Marshall, D. B., A critical evaluation of indentation techniques for measuring fracture toughness: II, Strength method. *J. Am. Ceramic Soc.*, **64**(9) (1991), 539–43.
13. Rice, R. W., Freiman, St. W. & Becher, P. F., Grain size dependence of fracture energy in ceramics; I, Experiment. *J. Am. Ceramic Soc.*, **64**(6) (1981) 345–55.
14. Rice, R. W. & Freiman, St. W., Grain size dependence of fracture energy in ceramics; II, A model for non-cubic materials. *J. Am. Ceramic Soc.*, **64**(6) (1981), 350–54.
15. Freiman, St. W. & Pohanka, R. C., Review of mechanically related failures of ceramics capacitors and capacitor materials. *J. Am. Ceramic Soc.*, **72**(12) (1989) 2258–63.
16. Buessem, W. R., Thermal shock testing. *J. Am. Ceramic Soc.*, **38**(1) (1955) 15–17.
17. Kingery, W. D., Factors affecting the thermal shock resistance of ceramic materials. *J. Am. Ceramic Soc.*, **38**(4) (1955) 3–15.
18. Hasselman, D. P. H., Unified theory of thermal shock fracture initiation and crack propagation in brittle ceramics. *J. Am. Ceram. Soc.*, **52**(11) (1969) 600–4.
19. Osterstock, F., Contact damage submitted to thermal shock: a method to evaluate and simulate thermal shock resistance of brittle materials. *Mat. Sci. Eng.*, **A168** (1993), 41–4.
20. Osterstock, F., Caplan, D. & Prouteau, C., Effect of thermal shock and related transient stresses on the stable and unstable extension of Vickers indentation cracks in brittle solids. *3. ECRS*, Vol. 3, eds P. Duran & J. F. Fernandez, 1993, pp. 997–1002.
21. Osterstock, F. & Moussa, R., Thermal shock resistance of ceramics: influence on fracture mechanical parameters. *Ceram. Forum Int.*, **3** (1988) 71–84.
22. Themines, D. & Osterstock, F., Linear non-elastic fracture mechanics: application on refractories. *2nd Int. Conf. on Residual Stresses, ICRS-2*, eds G. Beck, S. Denis & A. Simon, Elsevier Applied Science, 1989, pp. 985–90.
23. Kishimoto, A., Kounioto, K. & Yanagida, H., Mechanical and dielectric failure of $BaTiO_3$ ceramics. *J. Mat. Science*, **24** (1989) 698–702.
24. Chano, H. T., Shin, B. C. & Kim, H. G. Grain size dependence of electrically induced microcracking in ferroelectric ceramics. *J. Am. Ceram Soc.*, **72**(2) (1989) 327–9.
25. Davidge, R. W. & Tappin, G., Internal strain energy and the strength of brittle materials. *J. Mat. Science*, **3** (1968), 287–301.

26. Buresh, F. E., Fracture toughness testing of alumina. In *Fracture mechanics applied to brittle materials*, ed. St. W. Freiman. ASTM STP 678, 1979 pp. 151–65.
27. Kreher, W. & Pompe, W., Increased fracture toughness of ceramics by energy-dissipative mechanisms. *J. Mat. Science*, **16** (1981) 694–706.
28. Hutchinson, J. W., Crack tip shielding by microcracking in brittle solids. *Act. Metall.*, **35**(7) (1987) 1605–19.
29. Evans, A. G., Microfracture from thermal expansion anisotropy; I, Single phase system. *Acta Metall.*, **26** (1978), 1845–53.
30. Case, E. D., Smyth, J. R. & Hunter, O., Grain size dependence of microcrack initiation in brittle materials. *J. Mat. Science*, **15** (1980) 149–53.
31. Tvergaard, V. & Hutchinson, J. W., Microcracking in ceramics induced by thermal expansion or elastic anisotropy. *J. Am. Ceramic Soc.*, **71**(3) (1988) 157–66.